Displacement of P-Stereogenic Phosphiranes from Rhodium by CO in Hydroformylation Catalysis

Ryan M. Tipker,[a] Russell P. Hughes, [a] David S. Glueck, [a]* Heather A. Spinney, [b] Michael A. Brammer, [c] Arnold L. Rheingold [d]

[a] 6128 Burke Laboratory, Department of Chemistry, Dartmouth College, Hanover, New Hampshire 03755, United States [b] Dow, Core R&D, 1776 Building, 633 Washington St., Midland, Michigan 48667, United States [c] Dow, Industrial Solutions Process R&D, 2301 N. Brazosport Blvd., Freeport, Texas 77541, United States [d] Department of Chemistry, University of California, San Diego, 9500 Gilman Drive, La Jolla, California 92093, United States

ABSTRACT: The P-stereogenic phosphiranes *syn*- and *anti*-Mes*PCH_2CHPh (**1**-**2**, Mes* = 2,4,6-(*t*-Bu)$_3C_6H_2$) formed precatalysts for hydroformylation of propylene using the precursor Rh(acac)$(CO)_2$. Stoichiometric reactions gave the complexes Rh(acac)(L)(CO) (**3**-**4**). High-pressure NMR spectroscopy showed that Rh complex **3** was formed in the catalytic mixture, but on treatment with syngas (CO/H_2), the phosphirane was displaced from rhodium. These observations were consistent with a density functional theory (DFT) study, which found that the equilibrium between Rh(acac)$(CO)_2$, phosphiranes **1**-**2**, CO, and Rh(acac)(L)(CO) (**3**-**4**) favored the starting materials. These results emphasized the competition between CO and phosphine ligands for coordination to rhodium during hydroformylation, and the importance of strong Rh-L coordination to ensure control of catalyst properties.

1. INTRODUCTION

A variety of P-ligands have been tested to control activity and selectivity, especially the linear-branched ratio of the aldehyde products, in metal-catalyzed hydroformylation. Triphenylphosphine and bidentate bis(phosphites) have been particularly successful. Faster catalysis with phosphite ligands was ascribed to their π-acceptor properties, which promoted CO dissociation.[1] Because phosphiranes were also suggested, on the basis of Walsh diagram analysis, to be good π-acceptors,[2] they might behave similarly.[3] However, this idea has been little explored beyond a BASF patent on the use of Grützmacher's phosphirane BABAR-Phos (Chart 1) in Rh-catalyzed hydroformylation.[4] The P-N bond in BABAR-Phos and its bicyclic structure are unusual in phosphiranes,[5] so we wanted to test the simpler P-stereogenic phosphiranes *syn*- and *anti*-Mes*PCH_2CHPh (**1**-**2**)[6] which formed stable Vaska-type rhodium complexes *trans*-$RhL_2(CO)(Cl)$ (Mes* = 2,4,6-(*t*-Bu)$_3C_6H_2$, Chart 1).[7]

Experimental and computational evidence suggested that phosphiranes are slightly poorer σ-donors than the analogous phosphines, and, in contrast to the earlier hypothesis, their π-acceptor properties are similar.[7,8] These unusual ligands might therefore behave like "normal" phosphines in catalysis, but the three-membered ring causes significant differences which may limit their applications. Computational and calorimetric studies suggested that phosphines bind metals more strongly than do phosphiranes, which could result in ligand substitution and catalyst decomposition.[7,8] Strain in the phosphirane ring also resulted in metal-mediated ring opening, which was observed at the end of Rh(chiral phosphirane)-catalyzed asymmetric hydrogenation reactions,[9] or as a reversible process in Rh-BABAR-Phos complexes.[10]

Chart 1. Structures of BABAR-Phos, P-stereogenic phosphiranes **1**-**2**, and their Rh-Vaska complexes (Mes* = 2,4,6-(*t*-Bu)$_3C_6H_2$)

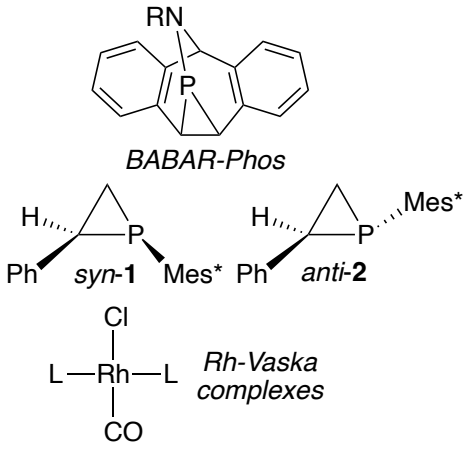

We hypothesized that the bulky Mes* group in phosphiranes **1**-**2** would prevent P-C cleavage, while using excess ligand might control catalyst speciation in equilibria with CO.[11] To further investigate the potential of phosphiranes as ligands in Rh-catalyzed hydroformylation, we report here the synthesis and structural characterization of catalyst precursors and application of these ligands under industrially relevant conditions. Studies of catalyst

speciation by high-pressure NMR spectroscopy showed that phosphirane **1** was displaced by CO, and density functional theory (DFT) calculations rationalized the thermodynamics of this process.

2. RESULTS AND DISCUSSION

The enantiomerically enriched phosphiranes (R_P,S_C)-*syn*-**1** and (R_P,R_C)-*anti*-**2** were tested in hydroformylation of propylene in a continuous reactor in tetraglyme at 75 °C, under pressure of 50 psi CO, 50 psi H_2 and 5 psi propylene (Scheme 1). The rhodium concentration was 100 ppm (0.91 mM, introduced to the reactor as $Rh(acac)(CO)_2$). Both ligands were tested at 10:1, 2:1, and 1:1 ligand to rhodium ratios. The reactions were run for 2-3 days, while continuously monitoring rate and linear/branched selectivity (n:i ratio) via on-line GC measurements (see the Supporting Information (SI) for details). The Rh/phosphirane mixtures were not very active or selective catalysts (turnover frequency (TOF) = 20-30/h for both ligands, n:i was 1.0-1.5). For comparison, under similar conditions, catalysis with PPh_3 was about ten times faster, with n:i of 1.9. Control experiments without added ligands showed that the presence of phosphiranes affected both catalytic rate and selectivity. Thus, over two days of operation, the average rate of catalysis with 2 equiv of phosphiranes **1** or **2** was about two times greater than for ligand-free $Rh(acac)(CO)_2$, and the average n:i ratio was also greater (1.3:1 for **1**, 1.2:1 for **2**, and 0.7:1 for the control).

Scheme 1. Hydroformylation of propylene using the catalyst precursor $Rh(acac)(CO)_2$ and *syn*- or *anti*-phosphiranes **1**-**2**

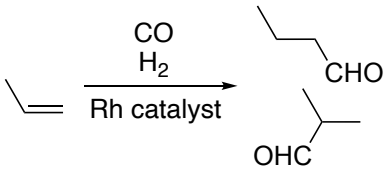

To investigate the structure of the active species under catalytic conditions, we first prepared Rh-phosphirane complexes by ligand substitution on $Rh(acac)(CO)_2$ using racemic **1** and **2** (Scheme 2). This process occurred smoothly with *syn*-phosphirane **1** to give **3**, but reaction of *anti*-phosphirane **2** to yield **4** was slow and required bubbling N_2 through the reaction mixture to remove CO. Complexes **3**-**4** were yellow solids whose NMR and IR spectra were similar to those of analogous Rh(acac)(L)(CO) complexes.[12] The CO stretching frequency of 1968 cm^{-1} for both **3**-**4** was in between the values for complexes where L is the powerful donor PAd_3 (Ad = 1-adamantyl, 1948 cm^{-1})[13] or the acceptor $P(NC_4H_4)_3$ (2012 cm^{-1}),[14] and similar to the $PPhMe_2$ complex (1971 cm^{-1}),[14] consistent with intermediate donor-acceptor properties of the phosphiranes.[7]

Scheme 2. Synthesis of Rh(acac)(L)(CO) complexes **3**-**4**

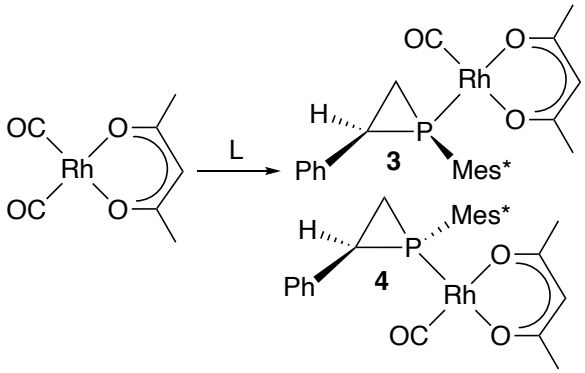

The crystal structure of *syn*-phosphirane complex **3** (Figure 1 and the SI) showed the expected square planar coordination at rhodium. The Rh-O1 distance trans to CO (2.041(2) Å) was shorter than the Rh-O2 bond length trans to the phosphirane (2.057(2) Å) and the analogous distance in $Rh(acac)(CO)(PPh_3)$ (2.087(4) Å), consistent with the trans influence order CO < *syn*-phosphirane **1** < PPh_3. Despite the bulk of the Mes* substituent, the Rh-P distance of 2.2339(8) Å in **3** was similar to the Rh-PPh_3 bond length of 2.244(2) Å.[15] As observed previously, upon complexation of phosphirane **1** to a metal, its P–C bonds shortened, and its angles at P increased.[7] The crystal structure of **3** was in good agreement with gas-phase density functional theory (DFT) calculations at the B3LYP-D3/LACV3P**++ level; see the SI for details.

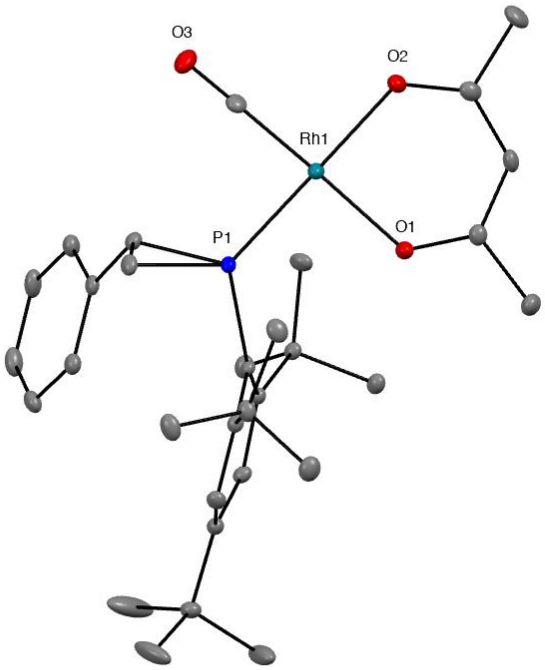

Figure 1. ORTEP diagram of Rh(acac)(CO)(*syn*-Mes*PCH_2CHPh) (**3**). Selected bond lengths (Å) and angles (deg): Rh-P 2.2339(8), Rh-O1 2.041(2), Rh-O2 2.057(2), Rh-C 1.813(3); O1-Rh-O2 90.10(9), O1-Rh-P 89.98(6), P-Rh-C 89.06(10), C-Rh-O2 91.02(11), O2-Rh-P 177.13(6), O1-Rh-C 176.58(11)

Consistent with these observations, when Rh(acac)$(CO)_2$ was treated with two equiv of *syn*-phosphirane **1** in d_8-toluene, gas evolution occurred, and the $^{31}P\{^1H\}$ NMR spectrum showed the formation of Rh complex **3** and unreacted ligand **1**. When the sample was pressurized in the high-pressure NMR reactor[16] to 300 psi with syngas (1:1 H_2:CO) and heated to 70 °C, with constant agitation of the sample by gas bubbles, $^{31}P\{^1H\}$ NMR spectroscopic monitoring showed disappearance of Rh complex **3** and an increase in the intensity of the signal due to free phosphirane **1**, which occurred within 10 minutes (Scheme 3, see the SI for details). There was no evidence for formation of the hydride complex Rh(L)$(CO)_2$(H), a commonly observed resting state in hydroformylation catalysis, either by ^1H or $^{31}P\{^1H\}$ NMR spectroscopy. These observations suggested that the phosphirane was displaced from Rh, and that the catalytic activity was due to Rh-carbonyl clusters formed from the Rh precursor, consistent with the limited dependence of activity and selectivity on the Rh/L stoichiometry or on the use of *syn*-**1** or *anti*-**2**. However, the increased rate and selectivity with these ligands, in comparison to the control experiment with the precursor Rh(acac)$(CO)_2$, implied that the phosphiranes still affected the catalytic cycle, perhaps in equilibria involving polynuclear Rh-CO complexes.

Scheme 3. Formation of Rh-phosphirane complex **3** and its decomposition under syngas in the high-pressure NMR reactor to regenerate **1** and unidentified Rh products ([Rh])

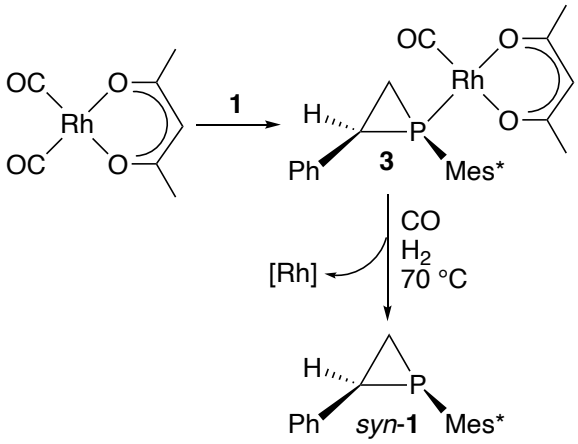

This ligand substitution under syngas pressure has been observed with several phosphines and phosphites, some of which are shown in Chart 2.[17] This competition between excess CO and the added ligand is often important, not just for bulky ligands. For example, even with excess PPh_3, phosphine-free Rh complexes were present during hydroformylation catalysis, as observed by high-pressure NMR and IR *operando* spectroscopy, and phosphite-CO coordination equilibria have also been observed.[18]

Chart 2. Selected phosphine and phosphite ligands which were displaced from rhodium under syngas pressure

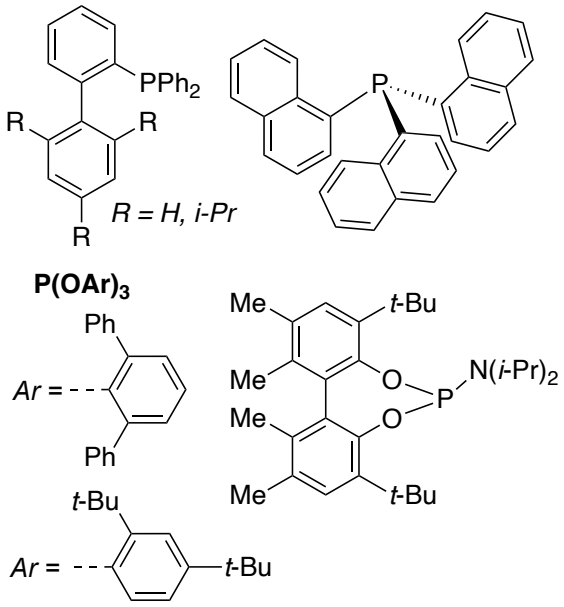

Such competition between CO and phosphines for coordination to the Rh(acac)(CO) fragment (Scheme 4) has been studied by solution calorimetry and by computation. The enthalpy of ligand substitution for the displacement of CO by PR_3 in CH_2Cl_2 at 30 °C ranged from −14.2 kcal/mol for PMe_2Ph to −2.4 kcal/mol for PPh_2(*o*-Tol).[14] Although the computed Gibbs free energy ΔG^{298K} for displacement of CO by PPh_3 at 25 °C was 1.3 kJ/mol, the success of the reaction was ascribed to loss of CO from the mixture.[19]

Scheme 4. Reversible ligand substitution by phosphines or phosphites (L) on Rh(acac)$(CO)_2$

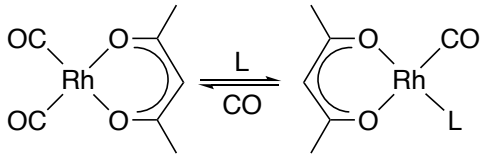

For comparison, our gas-phase DFT study found that displacement of CO by phosphiranes **1**-**2** to yield complexes **3**-**4** was thermodynamically unfavorable in both cases, by 1.9 kcal/mol for *syn*-**1** and by 5.9 kcal/mol for *anti*-**2**. This is consistent with the experimental observations, in which reaction of *anti*-**2** with Rh(acac)$(CO)_2$ to yield **4** required active removal of CO by bubbling N_2 through the reaction mixture. Presumably the sizable difference between the energies of complexes **3**-**4** is a steric effect stemming from an unfavorable interaction between the Rh(acac)(CO) fragment and the phosphirane phenyl substituent, although the computed Rh–P bond lengths of 2.295 Å for the two complexes were the same. We observed similar coordination behavior with a cyclometalated Pd complex, where *syn*-**1** bound irreversibly, while both free and bound *anti*-**2** were observed.[6]

With rhodium, the computed unfavorable thermodynamics of complex formation are consistent with the high-pressure NMR results, in which an excess of CO under syngas pressure rapidly displaced *syn*-phosphirane **1** from Rh complex **3**.

3. CONCLUSIONS

Rh-catalyzed hydroformylation is a particularly demanding application for phosphines, because "every ligand must compete with CO for coordination sites on the metal center."[1c] Here, although phosphiranes **1**-**2** formed the complexes Rh(acac)(CO)(phosphirane) (**3**-**4**), ligand **1** was displaced under syngas pressure, so the observed hydroformylation catalytic activity was apparently due to phosphine-free catalysts. However, the increased rate and selectivity compared to ligand-free conditions are consistent with some involvement of the phosphiranes in the catalytic cycle. To avoid this thermodynamically unfavorable coordination to Rh and the resulting inferior catalytic performance, bidentate bis(phosphiranes), which are very rare, are attractive targets for future testing, because the chelate effect should stabilize their complexes.[20]

4. EXPERIMENTAL SECTION

General Experimental Details The air-stable phosphiranes **1**-**2** and their Rh complexes **3**-**4** were handled in the air. Dichloromethane, dichloromethane-d_2, and pentane were dried over molecular sieves. Toluene-d_8 was purchased from Cambridge Isotope Labs and dried over activated 4 Å molecular sieves in a N_2-purged glove box. Routine NMR spectra were recorded with a 600 MHz spectrometer. ^{1}H or ^{13}C NMR chemical shifts are reported versus Me_4Si and were determined by reference to the residual ^{1}H or ^{13}C solvent peaks. ^{31}P NMR chemical shifts are reported versus H_3PO_4 (85%) used as an external reference. Coupling constants are reported in Hz, as absolute values. Unless indicated, peaks in NMR spectra are singlets. Atlantic Microlab (Norcross, GA) provided elemental analyses. Mass spectrometry was performed at the University of Illinois. Reagents were from commercial suppliers. Phosphiranes **1**-**2** were prepared by the literature method.[6]

Hydroformylation Catalysis The hydroformylation process was conducted in a glass pressure reactor operating in a continuous mode. The reactor consists of a three-ounce pressure bottle partially submerged in an oil bath (75 °C) with a glass front for viewing. Each reactor was charged with tetraglyme (20 mL) via syringe and purged with nitrogen overnight. Catalyst precursor solutions comprising rhodium (introduced as rhodium dicarbonyl acetylacetonate; 100 ppm) and ligand in toluene were then added. The catalyst solution was activated with a feed of 1:1 CO and H_2 at a total operating pressure of 150 psig (1034 kPa) for 30 to 60 minutes, and the reaction was subsequently initiated by the introduction of propylene. Flows of the individual gases were adjusted as desired, and nitrogen was added as necessary to maintain the desired total operating pressure of 150 psig (1034 kPa). The flows of the feed gases (H_2, CO, propylene, N_2) were controlled individually with mass flow meters and the feed gases were dispersed in the catalyst precursor solution via fritted metal spargers. The partial pressures of N_2, H_2, CO, propylene, and aldehyde products were determined by analyzing the vent stream by gas chromatographic (GC) analysis and Dalton's Law. The unreacted feed gases were stripped out along with the butyraldehyde products to maintain substantially constant liquid level. The outlet gas was analyzed periodically by GC. This equipment allows hydroformylation rate to be measured as a function of reaction temperature, CO and H_2 partial pressures, and Rh content.

Synthesis of Rh(acac)(CO)(*syn*-Mes*PCH$_2$CHPh) (3) A solution of crude *syn*-phosphirane in 0.5 mL of CD_2Cl_2 was added to Rh(acac)$(CO)_2$ (16.3 mg, 0.063 mmol). The reaction was monitored via ^{31}P{^{1}H} NMR spectroscopy, and more crude phosphirane was added until the Rh starting material was consumed; this required a total of 56 mg of crude ligand (nominally 0.15 mmol, 2.4 equiv). The solvent was removed under vacuum and the yellow residue was washed with cold pentane, then dried under vacuum, to give yellow blocky crystals (23 mg, 71% yield based on Rh). Slow evaporation of CH_2Cl_2 gave X-ray quality crystals.

Anal. Calcd for $C_{32}H_{44}O_3PRh$: C, 62.95; H, 7.26. Found: C, 63.01; H, 7.49. The parent ion was not observed by ESI-MS. ^{31}P{^{1}H} NMR (CD_2Cl_2): δ -93.9 (d, J = 220). ^{1}H NMR (CD_2Cl_2): δ 7.57 (1H, Ar CH), 7.03 (m, 2H, Ar CH), 6.94 (t, J = 8, 2H, Ar CH), 6.12 (br, 2H, Ar CH), 5.50 (1H, acac H), 2.95 (t, J = 10, 1H, CHPh), 2.14 (t, J = 10, 1H, CH_2), 2.06 (3H, acac CH_3), 1.82 (3H, acac CH_3), 1.81 (10H, 9H *t*-Bu plus 1H CH_2), 1.32 (9H, *t*-Bu), 1.22 (9H, *t*-Bu).^{13}C{^{1}H} NMR (CD_2Cl_2): δ 189.4 (dd, J = 28, 77, CO), 187.5 (quat acac), 185.5 (quat acac), 158.1 (d, J = 3, quat Ar), 158.0 (d, J = 6, quat Ar), 151.3 (quat Ar), 137.5 (d, J = 7, quat Ar), 127.6 (Ar CH), 127.5 (Ar CH), 125.9 (Ar CH), 125.4 (d, J = 8, Ar CH), 124.4 (d, J = 9, Ar CH), 100.5 (d, J = 2, acac CH), 40.5 (*C*Me$_3$), 40.2 (*C*Me$_3$), 35.1 (C*Me$_3$*), 34.7 (C*Me$_3$*), 34.6 (*C*Me$_3$), 32.2 (d, J = 14, CHPh), 30.9 (C*Me$_3$*), 27.3 (acac CH_3, overlapping), 27.2 (acac CH_3), 22.4 (d, J = 8, CH_2). One quat Ar peak was not observed.

Synthesis of Rh(acac)(CO)(*anti*-Mes*PCH$_2$CHPh) (4) A solution of *anti*-phosphirane (20.0 mg, 0.053 mmol, 1 equiv) in 0.5 mL of CD_2Cl_2 was added to Rh(acac)$(CO)_2$ (16.3 mg, 0.063 mmol, 1.18 equiv), and the reaction was monitored via ^{31}P{^{1}H} NMR spectroscopy. Conversion to the product was slow and incomplete, so N_2 was bubbled through the solution, with CH_2Cl_2 added when necessary to replace evaporated solvent. After 12 h of bubbling, removal of the solvent under vacuum gave a yellow solid (27 mg, 83%) which contained a small amount of Rh(acac)$(CO)_2$. This material was recrystallized from pentane at −20 °C to give a yellow solid (25 mg, 77% yield).

HRMS (ESI) calcd m/z 609.2005. Found m/z 609.1996. ^{31}P{^{1}H} NMR (CD_2Cl_2): δ −101.7 (d, J = 226). ^{1}H NMR (CD_2Cl_2): δ 7.53 (d, J = 8, 2H, Ar), 7.41 (dt, J = 2, 11, 2H, Ar), 7.30 (t, J = 7, 2H, Ar), 7.23 (t, J = 8, 1H, Ar), 5.47 (1H, acac), 2.83 (q, J = 9, 1H, CHPh), 2.04 (m, 1H, CH_2, overlapping), 2.03 (3H, CH_3), 1.85 (9H, CMe_3), 1.79 (3H, CH_3), 1.73 (9H, CMe_3), 1.59 (m, 1H, CH_2), 1.32 (9H, CMe_3). ^{13}C{^{1}H} NMR (CD_2Cl_2): δ 189.2 (dd, J = 75, 27, CO), 187.3 (quat acac), 185.1 (quat acac), 155.9 (apparent t, J = 5, 2 overlapping quat Ar), 150.7 (quat Ar), 137.8 (quat Ar), 128.9 (d, J = 6, Ar CH), 128.2 (Ar CH), 126.4 (Ar CH), 124.8 (d, J = 9, Ar CH), 124.1 (d, J = 8, Ar CH), 100.4 (d, J = 2, acac CH), 40.1 (*C*Me$_3$), 39.7 (*C*Me$_3$), 34.9

(d, J = 2, C*Me*$_3$), 34.7 (*C*Me$_3$), 34.2 (C*Me*$_3$), 33.0 (d, J = 10, CHPh), 31.3 (*C*Me$_3$), 30.8 (C*Me*$_3$), 27.1 (d, J = 6, acac CH$_3$), 26.9 (acac CH$_3$), 20.7 (d, J = 8, *C*H$_2$). One quat Ar signal was not observed.

High-pressure NMR High-pressure NMR experiments were performed in a Wisconsin High-Pressure NMR Reactor (WiHP-NMRR). The instrument was built at Dow based on a design from Clark Landis's research group at the University of Wisconsin.[16a] NMR spectra were collected on a Varian MR-400 MHz spectrometer with a 10 mm BB probe. Proton spectra were referenced to residual protio solvent. Phosphorus spectra were referenced to the corresponding proton spectrum using a VnmrJ macro.

In a N_2-purged glove box Rh(acac)(CO)$_2$ (24 mg, 0.093 mmol) was combined with phosphirane **1** (70 mg, 0.18 mmol, 2 equiv) in 1.5 mL of toluene-d$_8$. Gas evolution was noted from the yellow solution. The solution was pulled into a threaded, gas-tight syringe (syringe 1). A second gas-tight syringe was filled with 0.5 mL of toluene-d$_8$ (syringe 2, rinse). A third gas-tight syringe was filled with 1 mL of N_2 gas from the glove box atmosphere (syringe 3, N_2 chase).

The WiHP-NMRR was purged with nitrogen with three vent/refill cycles. The contents of syringe 1 were injected into the high-pressure NMR tube, followed by 0.5 mL of N_2 (syringe 3), 0.5 mL of toluene-d$_8$ (syringe 2), and then another 0.5 mL of N_2 (syringe 3). The reactor was pressurized with 50 psig of N_2, circulated for 30 s, and vented three times. Finally, the reactor was pressurized with 50 psig N_2, the sample was locked and shimmed, and ^{1}H and ^{31}P NMR spectra were collected.

The reactor was vented and then pressurized with 300 psig syngas (1:1 H_2:CO). The sample was locked and shimmed again at the higher pressure. The sample was then heated to 70 °C using the NMR probe heater. Gas was circulated continuously while collecting ^{31}P NMR spectra every 10 minutes for 1 hour. The gas circulation was turned off at the end of the experiment and a ^{1}H NMR spectrum was collected.

Supporting Information

Additional experimental details and NMR spectra (PDF)
Computed structures (xyz)

AUTHOR INFORMATION

Corresponding Author

* glueck@dartmouth.edu

ACKNOWLEDGMENT

We thank the National Science Foundation (CHE-1954412 and CHE-1562037) and the Polish National Alliance (scholarship for RMT) for support.

REFERENCES

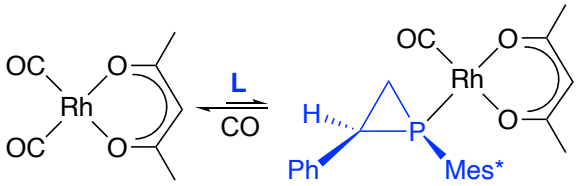

1. (a) van Leeuwen, P. W. N. M. Rhodium-Catalyzed Hydroformylation. In *Reference Module in Chemistry, Molecular Sciences and Chemical Engineering*, Elsevier, 2019. https://doi.org/10.1016/B978-0-12-409547-2.11261-2 (b) Franke, R.; Selent, D.; Borner, A. Applied Hydroformylation. *Chem. Rev.* **2012**, *112*, 5675-5732. (c) Zhang, B.; Peña Fuentes, D.; Börner, A. Hydroformylation. *ChemTexts* **2021**, *8*, 2.

2. Marinetti, A., Chiral Heterocyclic Phosphines. In *Phosphorus Ligands in Asymmetric Catalysis. Synthesis and Applications*, Börner, A., Ed. Wiley-VCH: Weinheim, 2008; Vol. 1, pp 114-135.

3. Liedtke, J.; Loss, S.; Widauer, C.; Grutzmacher, H. Phosphiranes as Ligands for Platinum Catalysed Hydrosilylations. *Tetrahedron* **2000**, *56*, 143-156.

4. Mackewitz, T.; Ahlers, W.; Paciello, R.; Gruetzmacher, H. Verfahren und Herstellung von Additionsprodukten ethylenisch ungesättigter Verbindungen. German patent DE 10215356 A1, 2002.

5. Glueck, D. S. Phosphiranes, Phosphirenes, and Heavier Analogues. In *Comprehensive Heterocyclic Chemistry IV*, Black, D. S., Cossy, J., Stevens, C. V. Eds.; Vol. 1; Elsevier, 2022; pp 464-505.

6. Muldoon, J. A.; Varga, B. R.; Deegan, M. M.; Chapp, T. W.; Eördögh, Á. M.; Hughes, R. P.; Glueck, D. S.; Moore, C. E.; Rheingold, A. L. Inversion of Configuration at the Phosphorus Nucleophile in Diastereoselective and Enantioselective Synthesis of P-Stereogenic syn-Phosphiranes from Chiral Epoxides. *Angew. Chem. Int. Ed.* **2018**, *57*, 5047–5051.

7. Deegan, M. M.; Muldoon, J. A.; Hughes, R. P.; Glueck, D. S.; Rheingold, A. L. Synthesis and Structure of Metal Complexes of P-Stereogenic Chiral Phosphiranes: An EDA-NOCV Analysis of the Donor–Acceptor Properties of Phosphirane Ligands. *Organometallics* **2018**, *37*, 1473–1482.

8. Laporte, C.; Frison, G.; Grutzmacher, H.; Hillier, A. C.; Sommer, W.; Nolan, S. P. Binding of Specialty Phosphines to Metals: Synthesis, Structure, and Solution Calorimetry of the Phosphirane Complex [$PtMe_2(^{iPr}$BABAR-Phos$)_2$]. *Organometallics* **2003**, *22*, 2202-2208.

9. Marinetti, A.; Mathey, F.; Ricard, L. Synthesis of Optically Active Phosphiranes and their Use as Ligands in Rhodium(I) Complexes. *Organometallics* **1993**, *12*, 1207-1212.

10. Liedtke, J.; Rüegger, H.; Loss, S.; Grützmacher, H. BABAR-Phos Rhodium Complexes: Reversible Metal Insertion into a Three-Membered Ring and Catalytic Hydroborations. *Angew. Chem., Int. Ed.* **2000**, *39*, 2478-2481.

11. Stanley, G. G. Reaction Mechanisms of Multistep Catalytic Cycles. In *Comprehensive Organometallic Chemistry III*, Mingos, D. M. P., Crabtree, R. H. Eds.; Elsevier, 2007; pp 119-140.

12. (a) Bonati, F.; Wilkinson, G. Dicarbonyl-β-diketonato- and related complexes of rhodium(I). *J. Chem. Soc.* **1964**, 3156-3160. (b) Trzeciak, A. M. M.; Ziółkowski, J. J. Infrared and NMR, ^{1}H, ^{19}F, ^{31}P studies of Rh(I) complexes of the formula: [Rh(β-diketone)$(CO)_x(P)_y$] (x = 0, 1, 2; y = 0, 1, 2; x + y = 2; P = PPh_3 or $P(OPh)_3$). *Inorg. Chim. Acta* **1985**, *96*, 15-20.

13. Chen, L.; Ren, P.; Carrow, B. P. Tri(1-adamantyl)phosphine: Expanding the Boundary of Electron-Releasing Character Available to Organophosphorus Compounds. *J. Am. Chem. Soc.* **2016**, *138*, 6392–6395.

14. Serron, S.; Huang, J.; Nolan, S. P. Solution Thermochemical Study of Tertiary Phosphine Ligand Substitution Reactions in the Rh(acac)(CO)(PR_3) System. *Organometallics* **1998**, *17*, 534-539.

15. Leipoldt, J. G.; Basson, S. S.; Bok, L. D. C.; Gerber, T. I. A. The crystal structure of acetylacetonatocarbonyltri-phenylphosphinerhodium(I). *Inorg. Chim. Acta* **1978**, *26*, L35-L37.

16. (a) Beach, N. J.; Knapp, S. M. M.; Landis, C. R. A reactor for high-throughput high-pressure nuclear magnetic resonance spectroscopy. *Rev. Sci. Instrum.* **2015**, *86*, 104101. (b) Brezny, A. C.; Landis, C. R. Development of a Comprehensive Microkinetic Model for Rh(bis(diazaphospholane))-Catalyzed Hydroformylation. *ACS Catal.* **2019**, 2501-2513.

17. (a) Kubis, C.; Ludwig, R.; Sawall, M.; Neymeyr, K.; Börner, A.; Wiese, K.-D.; Hess, D.; Franke, R.; Selent, D. A Comparative In Situ HP-FTIR Spectroscopic Study of Bi- and Monodentate Phosphite-Modified Hydroformylation. *ChemCatChem* **2010**, *2*, 287-295. (b) Rafter, E.; Gilheany, D. G.; Joost, N. H. R.; van Leeuwen, P. W. N. M. Rhodium-Catalyzed Hydroformylation Using Hindered Phosphine Ligands: An In Situ Study. *ChemCatChem* **2010**, *2*, 387-391. (c) Tricas, H.; Diebolt, O.; van Leeuwen, P. W. N. M. Bulky monophosphite ligands for ethene hydroformylation. *J. Catal.* **2013**, *298*, 198-205. (d) How, R. C.; Dingwall, P.; Hembre, R. T.; Ponasik, J. A.; Tolleson, G. S.; Clarke, M. L. Composition of catalyst resting states of hydroformylation catalysts derived from bulky mono-phosphorus ligands, rhodium dicarbonyl acetylacetonate and syngas. *Molec. Catal.* **2017**, *434*, 116-122.

18. (a) Bara-Estaún, A.; Lyall, C. L.; Lowe, J. P.; Pringle, P. G.; Kamer, P. C. J.; Franke, R.; Hintermair, U. Mapping catalyst activation, turnover speciation and deactivation in Rh/PPh_3-catalysed olefin hydroformylation. *Catal. Sci. Technol.* **2022**, *12*, 5501-5516. (b) Bara-Estaún, A.; Lyall, C. L.; Lowe, J. P.; Pringle, P. G.; Kamer, P. C. J.; Franke, R.; Hintermair, U. Multinuclear, high-pressure, operando FlowNMR spectroscopic study of Rh/PPh_3 – catalysed hydroformylation of 1-hexene. *Faraday Discussions* **2021**, *229*, 422-442. For related studies with phosphites, see: (c) Bara-Estaún, A.; Lyall, C. L.; Lowe, J. P.; Pringle, P. G.; Kamer, P. C. J.; Franke, R.; Hintermair, U. Understanding Rh-catalysed Hydroformylation with Phosphite Ligands through Catalyst Speciation Analysis by Operando FlowNMR Spectroscopy. *ChemCatChem* **2023**, *15*, e202201204. (d) Diebolt, O.; Tricas, H.; Freixa, Z.; van Leeuwen, P. W. N. M. Strong π-Acceptor Ligands in Rhodium-Catalyzed Hydroformylation of Ethene and 1-Octene: Operando Catalysis. *ACS Catal.* **2013**, *3*, 128-137.

19. Hopmann, K. H.; Conradie, J. Density Functional Theory Study of Substitution at the Square-Planar Acetylacetonato-dicarbonyl-rhodium(I) Complex. *Organometallics* **2009**, *28*, 3710-3715.

20. (a) Charrier, C.; Maigrot, N.; Mathey, F. Generation and chemical trapping of (1,2-ethanediphosphinidene)tetracarbonyl-tungsten. *Organometallics* **1987**, *6*, 586-591. (b) Vlaar, M. J. M.; Ehlers, A. W.; de Kanter, F. J. J.; Schakel, M.; Spek, A. L.; Lammertsma, K. Synthesis of a Complexed 2,2-Bisphosphirane. *Angew. Chem. Int. Ed.* **2000**, *39*, 2943-2945. (c) Vlaar, M. J. M.; Assema, S. G. A. v.; Kanter, F. J. J. d.; Schakel, M.; Spek, A. L.; Lutz, M.; Lammertsma, K. Metal-Template-Directed Synthesis of Diphosphorus Compounds through Intramolecular Phosphinidene Additions. *Chem. Eur. J.* **2002**, *8*, 58-65. (d) Abdel-Magied, A. F.; Majeed, M. H.; Abelairas-Edesa, M. F.; Ficks, A.; Ashour, R. M.; Rahaman, A.; Clegg, W.; Haukka, M.; Higham, L. J.; Nordlander, E. Synthesis and characterization of chiral phosphirane derivatives of $[(\mu\text{-H})_4Ru_4(CO)_{12}]$ and their application in the hydrogenation of an α,β-unsaturated carboxylic acid. *J. Organomet. Chem.* **2017**, *849–850*, 71–79.